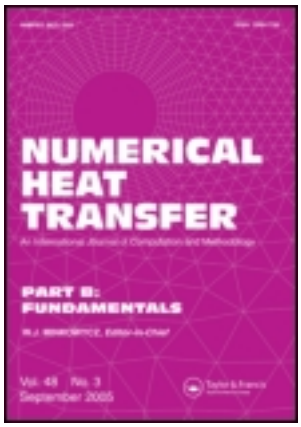

Numerical Heat Transfer, Part B: Fundamentals: An International Journal of Computation and Methodology
Publication details, including instructions for authors and subscription information:
http://www.tandfonline.com/loi/unhb20

USE OF THE MOMENTUM INTERPOLATION METHOD FOR NUMERICAL SOLUTION OF INCOMPRESSIBLE FLOWS IN COMPLEX GEOMETRIES: CHOOSING CELL FACE VELOCITIES

Seok Ki Choi [a] , Ho Yun Nam [a] & Mann Cho [a]
[a] Fast Breeder Reactor Coolant Department, Korea Atomic Energy Research Institute, P.O. Box 7, Daeduk-Danji, Daejon, 305-606, Korea
Version of record first published: 16 Apr 2007.

To cite this article: Seok Ki Choi , Ho Yun Nam & Mann Cho (1993): USE OF THE MOMENTUM INTERPOLATION METHOD FOR NUMERICAL SOLUTION OF INCOMPRESSIBLE FLOWS IN COMPLEX GEOMETRIES: CHOOSING CELL FACE VELOCITIES, Numerical Heat Transfer, Part B: Fundamentals: An International Journal of Computation and Methodology, 23:1, 21-41

To link to this article: http://dx.doi.org/10.1080/10407799308914888

Numerical Heat Transfer, Part B, vol. 23, pp. 21–41, 1993

USE OF THE MOMENTUM INTERPOLATION METHOD FOR NUMERICAL SOLUTION OF INCOMPRESSIBLE FLOWS IN COMPLEX GEOMETRIES: CHOOSING CELL FACE VELOCITIES

Seok Ki Choi, Ho Yun Nam, and Mann Cho
Fast Breeder Reactor Coolant Department, Korea Atomic Energy Research Institute, P.O. Box 7, Daeduk-Danji, Daejon 305-606, Korea

The momentum interpolation method developed by Rhie and Chow [1] is further refined and extended to employ the curvilinear covariant velocity components as cell face velocities. The related pressure–velocity coupling technique is described. The relative performances of the proposed scheme and of the scheme based on the contravariant cell face velocities are examined through applications to several test problems. The present scheme, based on the covariant cell face velocities, always provides simple and diagonal-dominant pressure and pressure-correction equations and shows good convergence and stability behavior even in a strongly nonorthogonal grid situation.

INTRODUCTION

In recent years, several calculation methods that employ nonorthogonal, body-fitted coordinates have been developed for better resolution of the flow field in domains of irregular geometries. The differences among these methods are the choice of dependent variables in the momentum equations, the grid arrangements, and the treatment of pressure–velocity coupling [1].

The dependent variables of the momentum equations in a general nonorthogonal coordinate system can be either Cartesian or curvilinear velocity components. When the Cartesian velocity components are selected as dependent variables in the momentum equations, the resulting conservation equations are simple, but both Cartesian velocity components should be stored at each cell face in order to compute the mass flux properly. Maliska and Raithby [2] developed such a calculation scheme employing the conventional staggered grid arrangement. Since the momentum equations for both Cartesian velocity components are solved at each of the cell faces, this scheme requires complex programming, computer storage, and computing time. However, a scheme that stores only one Cartesian velocity component at each cell face [3] will cause an undesired splitting of the pressure field when the flow direction deviates much from the direction of the velocity component stored at the cell face.

Relatively few attempts have been made to use the curvilinear covariant or contravariant velocity components as dependent variables in the momentum equations, since such schemes require complicated tensor algebra and the resulting governing equations

1040-7790/93 $10.00 + .00

NOMENCLATURE

A	coefficient in the discretization equation
b	source term in the discretization equation
b_j^i	geometric coefficients defined in Eq. (5)
D_j^i	geometric coefficients defined in Eqs. (6)–(7)
D_u^1, D_u^2	coefficients of pressure terms in Eq. (12)
D_v^1, D_v^2	coefficients of pressure terms in Eq. (13)
Du_ξ, Dv_η	coefficients of pressure terms in Eqs. (26)–(27)
D_U^1, D_U^2	coefficients of pressure terms in Eq. (32)
D_V^1, D_V^2	coefficients of pressure terms in Eq. (33)
f_e^+	geometric interpolation factor
J	Jacobian of the inverse coordinate transformation
p	pressure
p'	pressure correction
Re	Reynolds number
S	source term
S^P, S^C	linearized source terms
u, v	Cartesian velocity components
u_ξ, v_η	covariant velocity components
$\vec{\mathbf{u}}$	velocity vector
U, V	contravariant velocity components
α	relaxation factor or skewed angle
α_ξ, α_η, β_ξ, β_η	geometric coefficients defined in Eqs. (41)–(42)
Γ	diffusivity
ΔV	volume
μ	viscosity
ξ, η	axes of curvilinear coordinates
ρ	density
ϕ	transport variables

Superscripts

$n-1$	previous iteration level
u, v	pertaining to u and v velocity components

Subscripts

e, w, n, s	east, west, north, and south faces of a control volume
E, W, N, S	east, west, north, and south neighbors of the grid point P
p	pertaining to pressure
P	pertaining to the grid point P
u, v	pertaining to u and v velocity components
ϕ	pertaining to transport variable ϕ

involve curvature terms that usually tend to be ill-behaved unless the numerical grids are sufficiently smooth. Recently, Karki and Patankar [4] developed a calculation scheme to relieve these difficulties, in which the discretization equations and the source terms for the curvilinear covariant velocity components are obtained through algebraic manipulation of those terms based on the Cartesian velocity components.

In addition to the aforementioned staggered grid-based methods, Rhie and Chow [5] proposed a scheme based on the momentum interpolation method. In this scheme, the momentum equations are solved at cell-centered locations using the Cartesian velocity components as dependent variables, and the cell face velocities are obtained by interpolation of the momentum equations for the neighboring cell-centered Cartesian velocity components. A special kind of interpolation practice was devised to prevent the splitting of the pressure field.

However, the Rhie and Chow scheme did not take into account the presence of underrelaxation factors in the discretized momentum equations and neglected the effect of cross-derivative pressure terms in the evaluation of cell face contravariant velocities. Subsequent study by Peric [6] further refined the Rhie and Chow scheme, and Majumdar [7], Miller and Schmidt [8], and Rodi et al. [9] have removed the problem of relaxation factor dependency of the converged solution suffered in the original Rhie and Chow scheme.

Since the cell face velocities in Rhie and Chow's scheme are obtained explicitly by interpolation of neighboring cell-centered Cartesian velocity components, either Cartesian velocity components or curvilinear contravariant or covariant velocity components can be selected as cell face velocities without adding any significant complexity to the overall solution procedure. Different choices of cell face velocities lead to different treatments of the pressure–velocity coupling and thereby affect solution behavior. The use of Cartesian velocity components as cell face velocities requires more computer storage, since all Cartesian velocity components should be stored at each of the cell faces in order to evaluate the mass flux properly. This disadvantage is particularly grave in practical three-dimensional situations. The mass fluxes at the cell face locations may be adequately evaluated by employing the contravariant velocities as cell face velocities. However, this practice may result in complicated nine-point pressure and pressure-correction equations, which may lack diagonal dominance in a strongly nonorthogonal grid situation unless the cross-derivative pressure terms are treated by other means. The choice of covariant velocity components as cell face velocities always provides simple and diagonal-dominant pressure or pressure correction equations, although parts of mass fluxes at the cell faces are evaluated through interpolation of neighboring velocities.

In the present study, Rhie and Chow's scheme is further extended to employ both the contravariant and the covariant velocity components as cell face velocities to investigate how different choices of cell face velocities affect solution behavior. Two computer codes, based on the contravariant and on the covariant cell face velocities, are developed and are applied to several benchmark problems to evaluate their relative performance. The computed results are compared with available analytic solutions and with results from other calculation methods.

MATHEMATICAL FORMULATION

Governing Equations

The continuity equation and the conservation form of the transport equation for a general dependent variable ϕ in a generalized coordinate system (ξ, η) can be written as follows:

$$\frac{\partial}{\partial \xi}(\rho U) + \frac{\partial}{\partial \eta}(\rho V) = 0 \tag{1}$$

$$\frac{\partial}{\partial \xi}(\rho U\phi) + \frac{\partial}{\partial \eta}(\rho V\phi) = \frac{\partial}{\partial \xi}\left[\frac{\Gamma_\phi}{J}\left(D_1^1 \frac{\partial \phi}{\partial \xi} + D_2^1 \frac{\partial \phi}{\partial \eta}\right)\right] + \frac{\partial}{\partial \eta}\left[\frac{\Gamma_\phi}{J}\left(D_1^2 \frac{\partial \phi}{\partial \xi} + D_2^2 \frac{\partial \phi}{\partial \eta}\right)\right] + JS_\phi \tag{2}$$

where

$$U = b_1^1 u + b_2^1 v \tag{3}$$

$$V = b_1^2 u + b_2^2 v \tag{4}$$

and

$$b_1^1 = y_\eta \quad b_2^1 = -x_\eta \quad b_1^2 = -y_\xi \quad b_2^2 = x_\xi \tag{5}$$

$$D_1^1 = x_\eta^2 + y_\eta^2 \quad D_2^2 = x_\xi^2 + y_\xi^2 \tag{6}$$

$$D_2^1 = D_1^2 = -(x_\xi x_\eta + y_\xi y_\eta) \tag{7}$$

$$J = x_\xi y_\eta - x_\eta y_\xi \tag{8}$$

In these equations, ρ is the density of the fluid, Γ_ϕ is the diffusion coefficient of variable ϕ, (u, v) are the Cartesian velocity components in the (x, y) directions, and S_ϕ denotes the source term for the variable ϕ.

Discretization of Transport Equations

The computational domain is divided into quadrilateral control volumes and all Cartesian velocity components and scalar variables are solved at the geometric center of each control volume cell (Fig. 1). The discretization of the transport equations in the physical solution domain is performed using the finite-volume approach. The convection-diffusion terms are treated by the power-law profiles of Patankar [10]. The

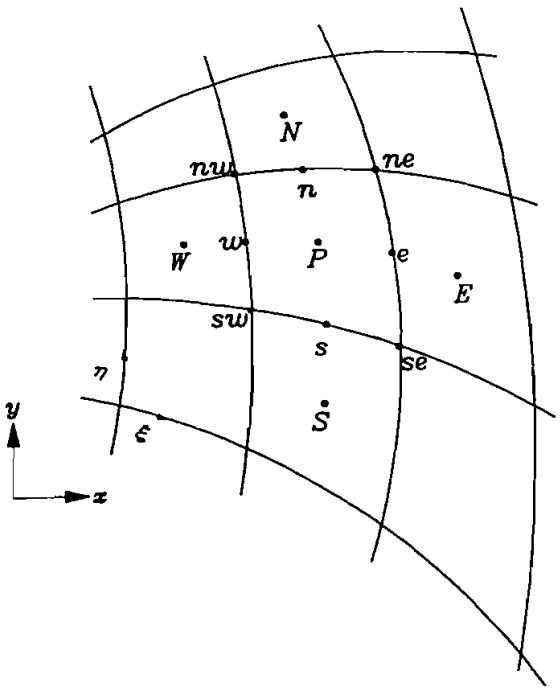

Fig. 1 A typical control volume.

resulting algebraic equations for a variable ϕ can be written in the following general form:

$$A_P\phi_P = A_E\phi_E + A_W\phi_W + A_N\phi_N + A_S\phi_S + b_\phi \tag{9}$$

where

$$A_P = A_E + A_W + A_N + A_S - S_\phi^P \Delta V \tag{10}$$

$$b_\phi = S_\phi^C \Delta V + S_\phi^b \tag{11}$$

S_ϕ^b is the source term of a variable ϕ arising due to the nonorthogonality of the numerical grid, and S_ϕ^C, S_ϕ^P are the linearized source terms.

The Momentum Interpolation Method

In Rhie and Chow's scheme, the momentum equations are solved implicitly at the cell-centered locations. The discretized form of momentum equations for the cell-centered, Cartesian velocity components can be written as follows with the underrelaxation factor expressed explicitly:

$$u_P = (H_u)_P + (D_u^1)_P(p_w - p_e) + (D_u^2)_P(p_s - p_n) + (1 - \alpha)u_P^{n-1} \tag{12}$$

$$v_P = (H_v)_P + (D_v^1)_P(p_w - p_e) + (D_v^2)_P(p_s - p_n) + (1 - \alpha)v_P^{n-1} \tag{13}$$

where

$$H_u = \frac{\alpha(\sum_{nb} A_{nb}^u u_{nb} + b_u)}{A_P^u} \tag{14}$$

$$H_v = \frac{\alpha(\sum_{nb} A_{nb}^v v_{nb} + b_v)}{A_P^v} \tag{15}$$

and

$$D_u^1 = \frac{\alpha b_1^1}{A_P^u} \quad D_u^2 = \frac{\alpha b_1^2}{A_P^u} \quad D_v^1 = \frac{\alpha b_2^1}{A_P^v} \quad D_v^2 = \frac{\alpha b_2^2}{A_P^v} \tag{16}$$

In these equations, α is the underrelaxation factor and the superscript $(n - 1)$ denotes the previous iteration level.

The momentum equations for the Cartesian velocity components at the cell face locations can be written as follows:

$$u_e = (H_u)_e + (D_u^1)_e(p_P - p_E) + (D_u^2)_e(p_{se} - p_{ne}) + (1 - \alpha)u_e^{n-1} \tag{17}$$

$$v_e = (H_v)_e + (D_v^1)_e(p_P - p_E) + (D_v^2)_e(p_{se} - p_{ne}) + (1 - \alpha)v_e^{n-1} \tag{18}$$

and

$$u_n = (H_u)_n + (D_u^1)_n(p_{wn} - p_{en}) + (D_u^2)_n(p_P - p_N) + (1 - \alpha)u_n^{n-1} \tag{19}$$

$$v_n = (H_v)_n + (D_v^1)_n(p_{wn} - p_{en}) + (D_v^2)_n(p_P - p_N) + (1 - \alpha)v_n^{n-1} \tag{20}$$

In the present modified Rhie and Chow scheme, these cell face Cartesian velocity components are obtained through interpolation of the momentum equations for the neighboring cell-centered Cartesian velocity components. The following assumptions are introduced in the present study to evaluate cell face velocities such as u_e at the east cell face:

$$\frac{1}{(A_P^u)_e} \simeq \frac{f_e^+}{(A_P^u)_E} + \frac{(1 - f_e^+)}{(A_P^u)_P} \tag{21}$$

$$(H_u)_e \simeq f_e^+(H_u)_E + (1 - f_e^+)(H_u)_P \tag{22}$$

where f_e^+ is the geometric interpolation factor and is defined in terms of distances between nodal points,

$$f_e^+ = \frac{\overline{Pe}}{\overline{Pe} + \overline{eE}} \tag{23}$$

Similar assumptions can be introduced for the evaluation of the other cell face velocities, v_e and (u_n, v_n). The assumptions introduced in the present study are similar to those reported in previous works [6–9, 11]. Note that the momentum equations for the cell face velocities that incorporate their relations with the cell-centered velocities can be derived in a quite different manner [12].

The momentum equations for the curvilinear velocity components at the cell face locations are obtained through algebraic manipulation of the momentum equations for the cell face Cartesian velocity components.

The covariant velocity components (u_ξ, v_η) are related to the Cartesian velocity components (u, v) as

$$u_\xi = \bar{\mathbf{e}}_\xi \cdot \bar{\mathbf{u}} = \frac{x_\xi u + y_\xi v}{(x_\xi^2 + y_\xi^2)^{1/2}} \tag{24}$$

$$v_\eta = \bar{\mathbf{e}}_\eta \cdot \bar{\mathbf{u}} = \frac{x_\eta u + y_\eta v}{(x_\eta^2 + y_\eta^2)^{1/2}} \tag{25}$$

where $\bar{\mathbf{e}}_\xi$, $\bar{\mathbf{e}}_\eta$ are the unit vectors in the ξ, η directions. The momentum equations for the cell face covariant velocity components can be obtained by substituting Eqs. (17)–(20) into Eqs. (24)–(25). The resulting equations can be written as

$$(u_\xi)_e = (H_{u_\xi})_e + (Du_\xi)_e(p_P - p_E) + (1 - \alpha)(u_\xi^{n-1})_e \tag{26}$$

$$(v_\eta)_n = (H_{v_\eta})_n + (Dv_\eta)_n(p_P - p_N) + (1 - \alpha)(v_\eta^{n-1})_n \tag{27}$$

where

$$H_{u_\xi} = \frac{x_\xi H_u + y_\xi H_v}{(x_\xi^2 + y_\xi^2)^{1/2}} \tag{28}$$

$$H_{v_\eta} = \frac{x_\eta H_u + y_\eta H_v}{(x_\eta^2 + y_\eta^2)^{1/2}} \tag{29}$$

and

$$Du_\xi = \frac{x_\xi D_u^1 + y_\xi D_v^1}{(x_\xi^2 + y_\xi^2)^{1/2}} \tag{30}$$

$$Dv_\eta = \frac{x_\eta D_u^2 + y_\eta D_v^2}{(x_\eta^2 + y_\eta^2)^{1/2}} \tag{31}$$

The momentum equations for the physical contravariant cell face velocities (volume fluxes), defined in Eqs. (3)–(4), can be derived in a similar manner.

$$U_e = (H_U)_e + (D_U^1)_e(p_P - p_E) + (D_U^2)_e(p_{se} - p_{ne}) + (1 - \alpha)U_e^{n-1} \tag{32}$$

$$V_n = (H_V)_n + (D_V^1)_n(p_{wn} - p_{en}) + (D_V^2)_n(p_P - p_N) + (1 - \alpha)V_n^{n-1} \tag{33}$$

where

$$H_U = (b_1^1 H_u + b_2^1 H_v) \tag{34}$$

$$H_V = (b_1^2 H_u + b_2^2 H_v) \tag{35}$$

and

$$D_U^1 = (b_1^1 D_u^1 + b_2^1 D_v^1) \qquad D_U^2 = (b_1^1 D_u^2 + b_2^1 D_v^2) \tag{36}$$

$$D_V^1 = (b_1^2 D_u^1 + b_2^2 D_v^1) \qquad D_V^2 = (b_1^2 D_u^2 + b_2^2 D_v^2) \tag{37}$$

These cell face curvilinear velocity components are evaluated explicitly using the assumptions given in Eqs. (21)–(22) with the geometric coefficients evaluated at the cell face locations.

Treatment of Pressure–Velocity Coupling

In the present study, the coupling between the continuity and the momentum equations is effected using the SIMPLE algorithm [10]. Following are details of the pressure-

correction scheme associated with employing the covariant velocity components as cell face velocities, which are similar to those reported in Karki and Patankar [4], who used the conventional staggered grid method.

The integrated continuity equation for a control volume around a grid point P (Fig. 1) can be written as

$$(\rho U)_e - (\rho U)_w + (\rho V)_n - (\rho V)_s = 0 \tag{38}$$

The physical contravariant velocity components can be expressed in terms of the covariant velocity components as

$$U = \alpha_\xi u_\xi - \beta_\xi v_\eta \tag{39}$$

$$V = \alpha_\eta v_\eta - \beta_\eta u_\xi \tag{40}$$

where α_ξ, α_η, β_ξ, β_η are the geometric coefficients defined as

$$\alpha_\xi = \frac{D_1^1 (D_2^2)^{1/2}}{J} \qquad \beta_\xi = -\frac{D_1^2 (D_1^1)^{1/2}}{J} \tag{41}$$

$$\alpha_\eta = \frac{D_2^2 (D_1^1)^{1/2}}{J} \qquad \beta_\eta = -\frac{D_1^2 (D_2^2)^{1/2}}{J} \tag{42}$$

With these relations, the continuity equation can be written as

$$(\rho\alpha_\xi u_\xi)_e - (\rho\alpha_\xi u_\xi)_w + (\rho\alpha_\eta v_\eta)_n - (\rho\alpha_\eta v_\eta)_s = b_{NO} \tag{43}$$

where b_{NO} is source term arising due to the choice of covariant velocity components as cell face velocities and is defined as

$$b_{NO} = (\rho\beta_\xi v_\eta)_e - (\rho\beta_\xi v_\eta)_w + (\rho\beta_\eta u_\xi)_n - (\rho\beta_\eta u_\xi)_s \tag{44}$$

It was observed that the accuracy of the converged solution, especially in a coarse grid situation, is influenced a little by the way of evaluating the nonorthogonal mass source term, b_{NO} in Eq. (44). Our numerous numerical experiments in various situations show that it is better to evaluate the b_{NO} term through interpolation of neighboring updated [by Eqs. (51)–(52)] Cartesian velocity components rather than through the neighboring covariant velocity components. For example, the v_η velocity component at the east cell face location is evaluated through the relation given in Eq. (25) with the geometric coefficients evaluated there and the following simple interpolation

$$u_e \simeq f_e^+ u_E + (1 - f_e^+) u_P \qquad v_e \simeq f_e^+ v_E + (1 - f_e^+) v_P \tag{45}$$

This practice does not require the specification of inconvenient boundary conditions for the covariant velocity components.

The covariant cell face velocity components obtained by Eqs. (26)–(27) generally

will not satisfy mass conservation unless the pressure field is correct. These starred velocity components are corrected to satisfy the continuity equation by the following velocity correction equations:

$$(\Delta u_\xi)_e = (u_\xi - u_\xi^*)_e = (Du_\xi)_e(p'_P - p'_E) \tag{46}$$

$$(\Delta v_\eta)_n = (v_\eta - v_\eta^*)_n = (Dv_\eta)_n(p'_P - p'_N) \tag{47}$$

where p' is the pressure correction.

Substitution of these velocity-correction formulas into the continuity equation, Eq. (43), results in an equation for pressure correction:

$$A_P p'_P = \sum_{nb} A_{nb} p'_{nb} + b_C + b_{NO} \tag{48}$$

where

$$b_C = (\rho\alpha_\xi u_\xi^*)_w - (\rho\alpha_\xi u_\xi^*)_e + (\rho\alpha_\eta v_\eta^*)_s - (\rho\alpha_\eta v_\eta^*)_n \tag{49}$$

After solving the above pressure-correction equation, the pressure and the cell-centered Cartesian velocity components are updated by the following equations:

$$p = p^* + \alpha_P p' \tag{50}$$

$$u_P = u_P^* + (D_u^1)_P (P'_w - P'_e) + (D_u^2)_P (P'_s - P'_n) \tag{51}$$

$$v_P = v_P^* + (D_v^1)_P (P'_w - P'_e) + (D_v^2)_P (P'_s - P'_n) \tag{52}$$

The above velocity-correction equations for the cell-centered Cartesian velocity components are derived assuming a linearly varying pressure field.

The pressure-correction scheme associated with employing the contravariant velocity components as cell face velocities can be derived in a similar manner and is reported in previous works [6, 9, 11]. The details are not reproduced here, but the nonorthogonal pressure-correction terms appearing in the correction equations for the contravariant cell face velocity components are neglected in the present study to avoid a complicated nine-point pressure-correction equation. As will be shown later, this simplification of the pressure-correction equation leads to poor convergence as well as unstable solution behavior when the numerical grids are strongly nonorthogonal.

DISCUSSION OF THE MOMENTUM INTERPOLATION METHOD

A closer examination of the present Rhie and Chow scheme reveals that the cell-centered Cartesian velocity components that satisfy the momentum equations only satisfy the continuity equation with the assumption of a linearly varying pressure field, Eqs. (51)–(52). There is no strict way of enforcing mass conservation for the cell-centered velocity components. The cell face velocities satisfy the continuity equation, but they are evaluated from the averaged momentum equations based on the assump-

tions given in Eqs. (21)–(22). Therefore, the success of Rhie and Chow's scheme leans heavily on the validity of these assumptions. When these assumptions are not appropriate for a certain flow region, the scheme may result in a strange converged solution in which the cell-centered velocities and the cell face velocities converge to different values. Miller and Schmidt [8] found that such physically unrealistic solutions may occur in regions of strongly varying pressure gradient. They also observed that these physically unrealistic solutions do not differ substantially from the physically realistic limits, nor do they appear to have any noticeable effects on the overall solution process. Their observation has been reconfirmed by the recent study of Kobayashi and Pereira [13]. In the conventional staggered arrangements, the velocity components exactly satisfy the continuity equation and the momentum equations and do not cause these problems.

As shown in Eqs. (17)–(20), the momentum equations for the cell face velocity components in Rhie and Chow's scheme are based on exactly the same equations as are employed in the conventional staggered grid method. In the conventional staggered grid method, the momentum equations for the cell face velocity components are solved at the cell face locations with the algebraic coefficients evaluated there. However, the cell face velocities in the present Rhie and Chow scheme are evaluated explicitly through interpolation of the momentum equations for the cell-centered velocity components (*momentum interpolation method*). The main difference between the present Rhie and Chow scheme and the conventional staggered grid method is the way of handling the momentum equations for the cell face velocity components, and other details are redundant. Equations (17)–(20) also indicate that the cell face velocity components should be stored in order to obtain a relaxation factor–independent solution, implying that the staggering idea is adopted in this scheme. Therefore, it would be appropriate to say that Rhie and Chow's scheme is a staggered grid method based on momentum interpolation for velocities, Eqs. (21)–(22), and linear interpolation for pressure, Eqs. (51)–(52). For incompressible flow calculations with primitive variable formulation, the staggering is inevitable and the main focus of the scheme should be the treatment of the cell face velocities, not the cell-centered velocities. Majumdar et al. [14] have presented an excellent discussion on this argument.

It is also worthwhile to mention that the recently developed control-volume-based finite-element methods [15–17] resemble the present Rhie and Chow scheme in many respects. However, none of these schemes store velocity components at the cell-face locations, nor do they take into account the presence of relaxation factors in the discretized momentum equations for the cell face velocity components. Therefore, it is questionable whether such schemes may result in relaxation factor–independent converged solutions.

APPLICATIONS TO TEST PROBLEMS

Two computer codes based on the present modified Rhie and Chow scheme with different cell face velocities, one with contravariant velocity components [ELCON2D] and the other with covariant velocity components [ELCOV2D], are developed and are applied to several test problems to validate the solution procedures as well as to assess their relative performance. The test problems include laminar flow through a gradual expansion, fully developed laminar flow in a plane channel, and laminar flow in a lid-

driven cavity. The computed results are compared with the analytic solution and with those from other calculation methods.

Laminar Flow Through a Gradual Expansion

This problem was a test problem for the fifth workshop of the International Association for Hydraulic Research (IAHR) Working Group on Refined Modelling of Flow [18]. The geometry of the problem and the grid lines generated are shown in Fig. 2. This problem was solved for Reynolds numbers of 10 and 100 using 21 × 21 uniform grids.

The convergence histories of the sum of the normalized mass residuals of the

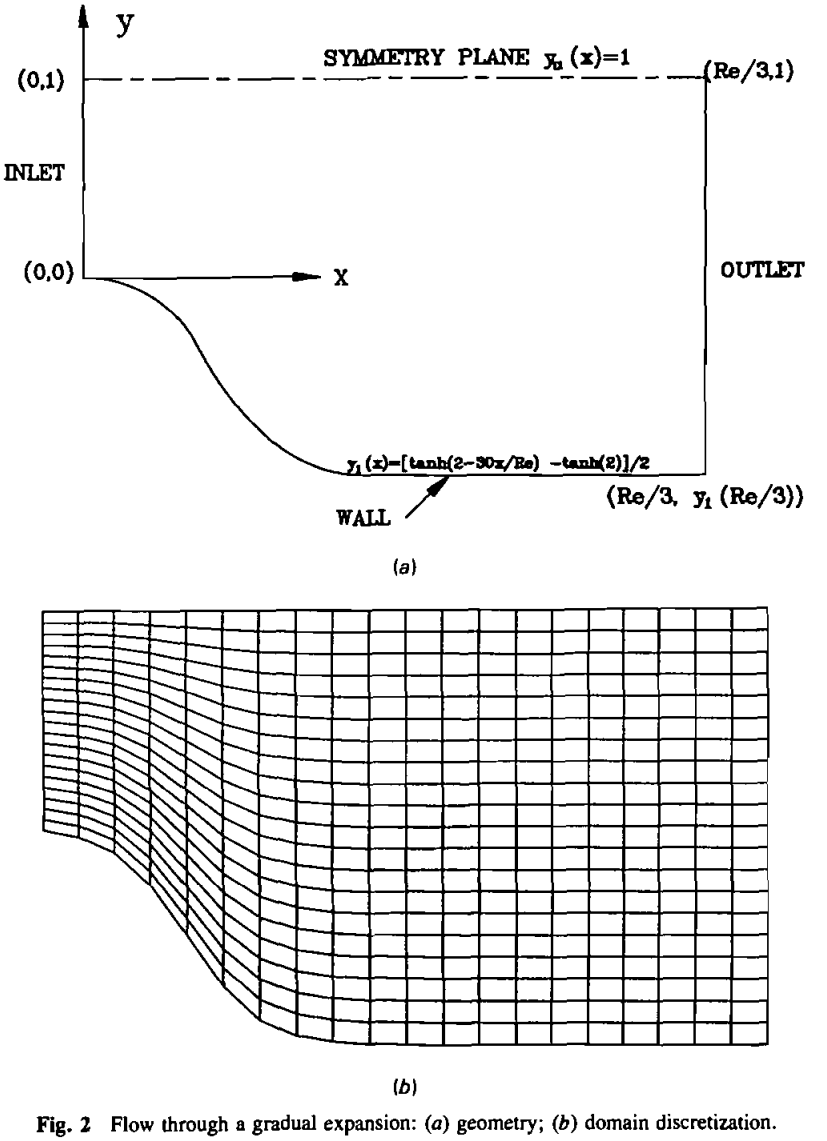

Fig. 2 Flow through a gradual expansion: (*a*) geometry; (*b*) domain discretization.

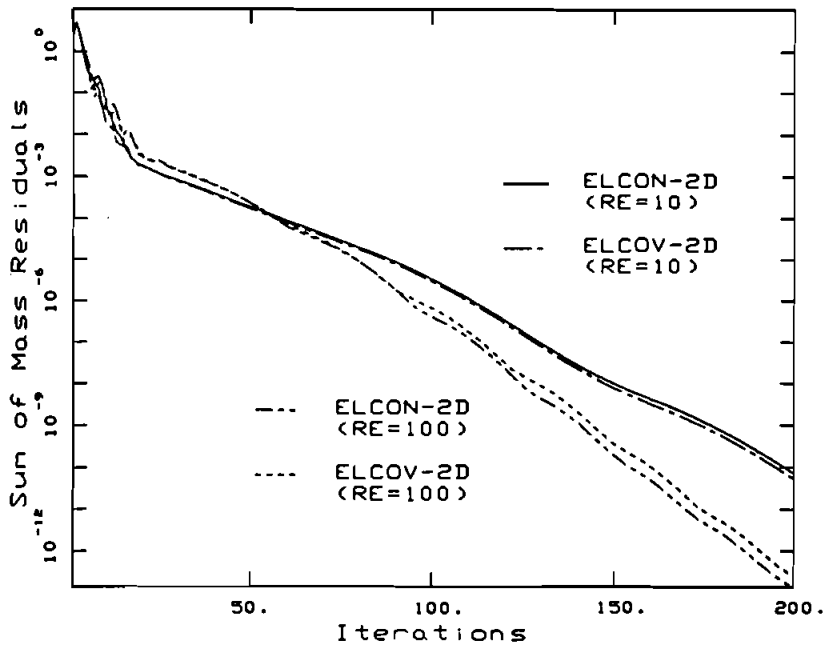

Fig. 3 Convergence histories.

pressure correction equation are shown in Fig. 3. As shown in this figure, the different choices of cell face velocities in Rhie and Chow's scheme do not affect the convergence behavior in this moderately nonorthogonal grid situation. The predicted wall surface pressure and vorticity distributions are shown in Figs. 4 and 5 together with other predicted results presented at that workshop and those by Karki [1]. The solution designated as C.J.G is considered to be a grid-independent solution by Cliffe et al. in Ref. [18] using the finite-element method with primitive variable formulation. The solution D.G designates the numerical solutions obtained by Demirovic and Gosman in Ref. [18] using the finite-volume method. The accuracy of the numerical solution is not influenced by the choice of cell face velocities. Although some differences are observed due to the use of a relatively coarse grid, both the present results compare favorably with the benchmark solution by Cliffe et al. in Ref. [18]. It is observed that the present solutions are a little sensitive to the geometric shape compared with other solutions by the conventional staggered grid method. However, Fig. 6 shows that the accuracy of the present solutions can be much improved with a little grid refinement (41 × 21).

Fully Developed Channel Flow

Fully developed laminar flow in a plane channel with a Reynolds number (Re = $\rho u_{ref} H/\mu$) of 100 is solved with various degrees of nonorthogonality of the numerical grid. The uniform 21 × 21 grids are generated within a solution domain that extends to five times the half-width of the channel, as shown in Fig. 7. Exact fully developed profiles are prescribed at the inlet, and zero axial gradient conditions are imposed at the exit.

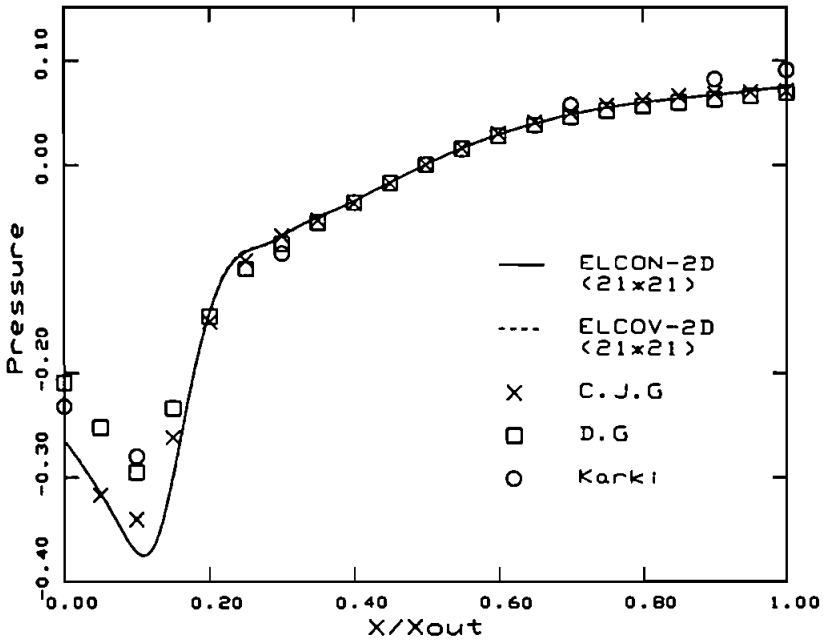

(*a*)

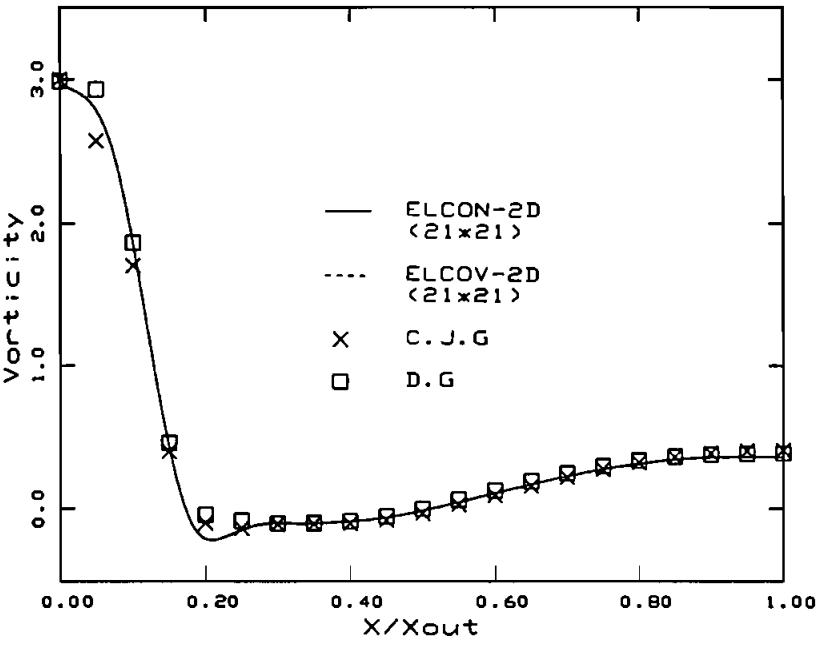

(*b*)

Fig. 4 (*a*) Wall pressure and (*b*) vorticity distributions: Re = 10, 21 × 21 grid.

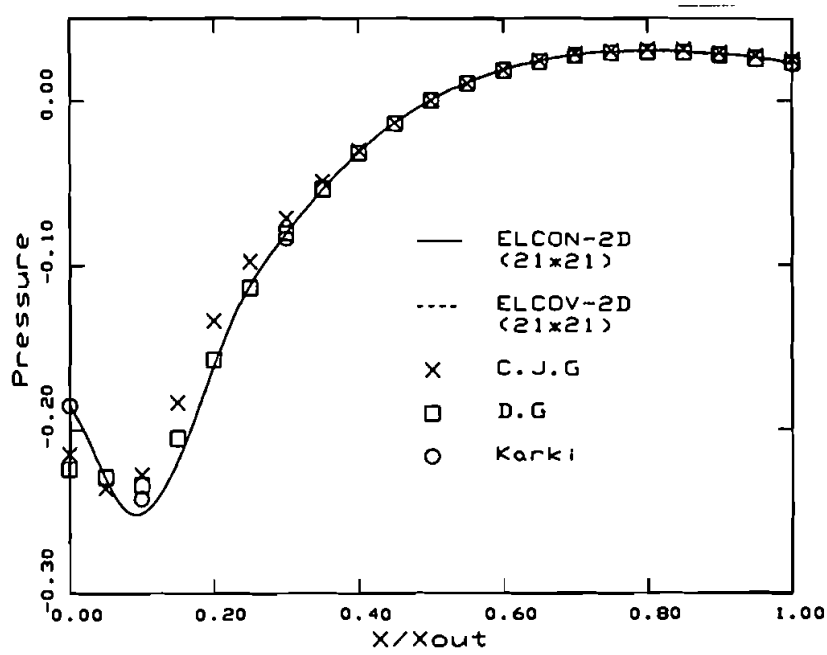

(*a*)

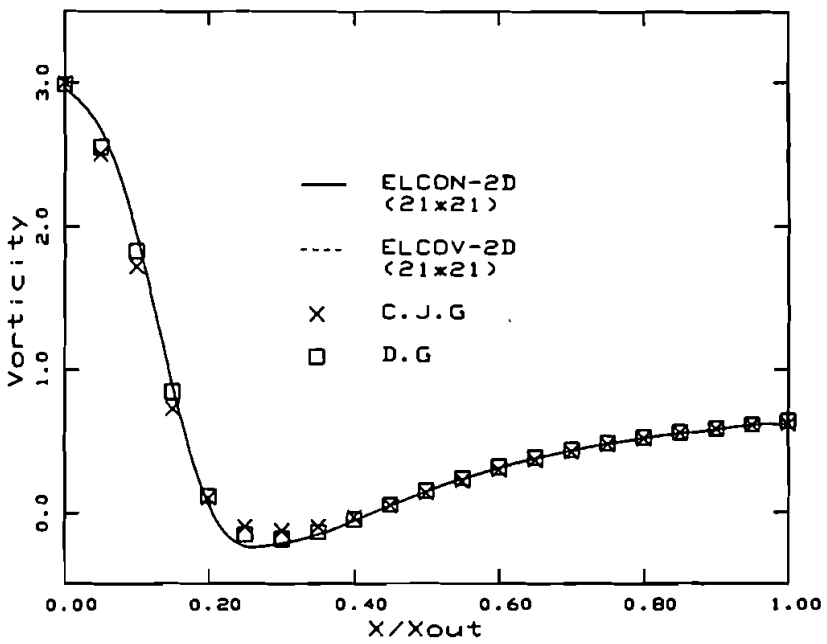

(*b*)

Fig. 5 (*a*) Wall pressure and (*b*) vorticity distributions: Re = 100, 21 × 21 grid.

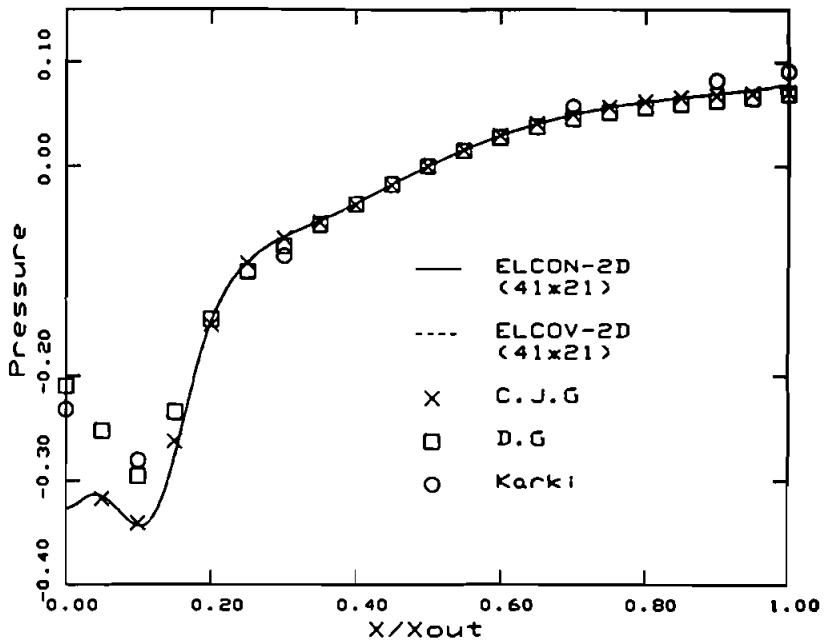

(a)

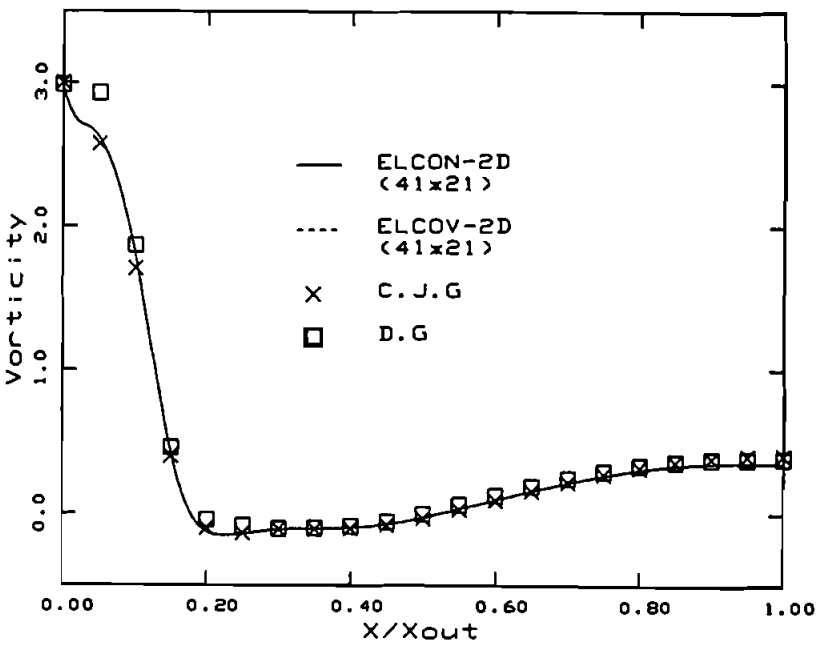

(b)

Fig. 6 (*a*) Wall pressure and (*b*) vorticity distributions: Re = 10, 41 × 21 grid.

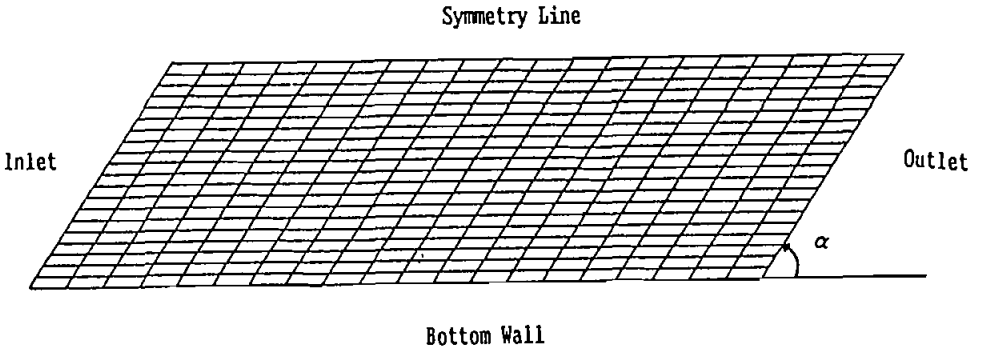

Fig. 7 Fully developed channel flow: Geometry and domain discretization.

Figure 8 shows that the convergence rates are influenced by the degree of nonorthogonality of the numerical grid as well as by the choice of cell face velocities when the numerical grids are strongly nonorthogonal ($\alpha = 45°$). In a strongly nonorthogonal grid situation ($\alpha = 45°$), the calculation by the ELCON2D code shows a slower convergence due to the neglect of nonorthogonal pressure-correction terms in the contravariant velocity-correction equations to provide a simple and diagonal-dominant pressure-correction equation. As shown in Table 1, the accuracy of the converged solution is not affected by the choice of cell face velocities. The maximum percentage error, E_{max} in Table 1, is defined as $E_{max} = 100 \times | u_{cal} - u_{exact} |_{max}/u_{ref}$, where the reference velocity u_{ref} is the average inlet velocity. The maximum percentage error

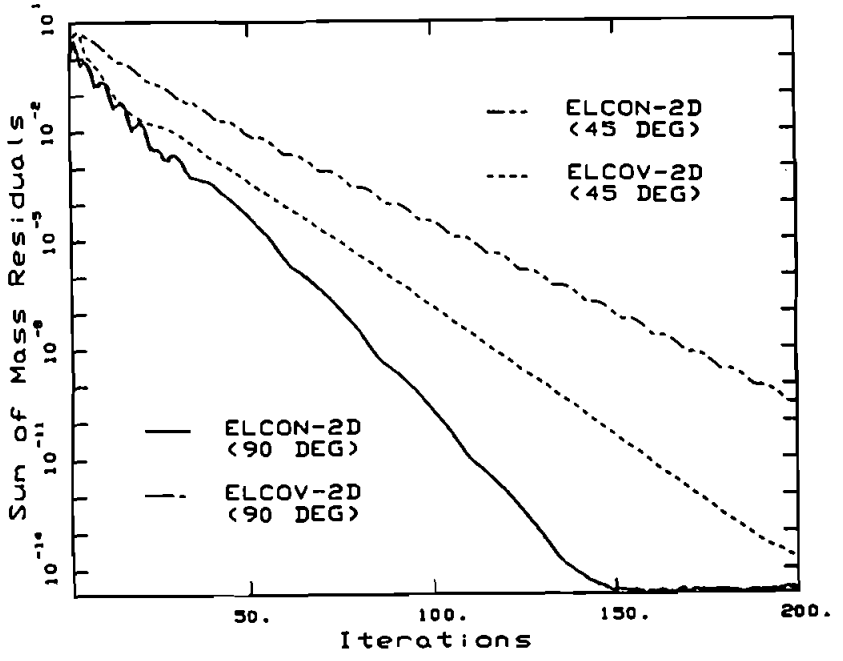

Fig. 8 Convergence histories.

Table 1 Maximum Percentage Errors of u Velocity Component

Code	$\alpha = 90°$	$\alpha = 60°$	$\alpha = 45°$
ELCON2D	0.123	1.565	3.094
ELCOV2D	0.123	1.565	3.094

becomes larger with increasing grid nonorthogonality, and nonnegligible errors are observed when the numerical grids are strongly nonorthogonal ($\alpha = 45°$). However, most maximum errors occurred at the last few stations near the outlet and, except for these regions, the maximum errors are less than 1%. These observations indicate that the maximum numerical errors are somewhat related to the treatment of boundary conditions at the exit.

Flow in a Lid-Driven Cavity

Fluid flow in a cavity with a moving wall and inclined side walls, shown schematically in Fig. 9, is solved to investigate the effects of nonorthogonality of the numerical grid on the convergence and the stability of the solutions. Four cases with different inclinations ($\alpha = 90°, 60°, 45°, 30°$) are studied employing 21 × 21 uniform numerical grids. The Reynolds number ($\mathrm{Re} = \rho U_0 L/\mu$) is fixed at 100 in all cases.

Figure 10 shows the convergence histories of the sums of the normalized mass residuals of the pressure-correction equation for four cases with different inclinations. When the numerical grids are orthogonal ($\alpha = 90°$), both codes result in the same convergence histories, as expected. As the grid nonorthonality becomes more significant, the differences in the convergence rates associated with employing different cell face velocities become more pronounced. The ELCOV2D code, based on the covariant cell face velocities, always shows better convergence behavior. When the numerical

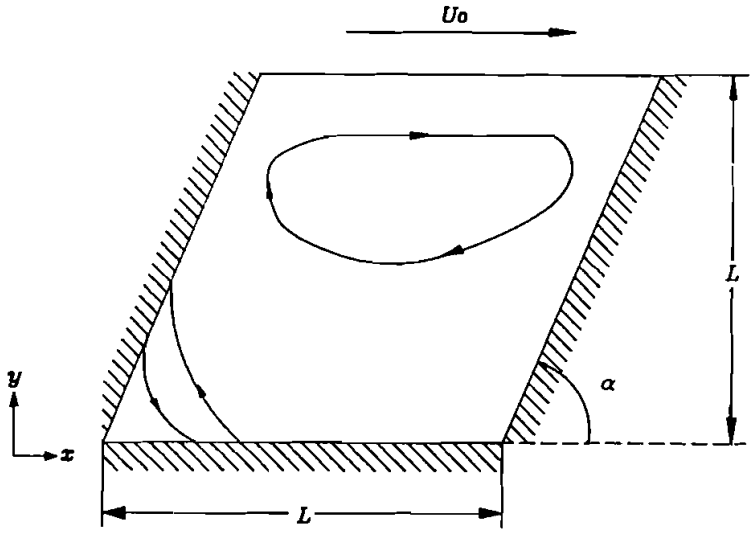

Fig. 9 Lid-driven cavity flow: Geometry.

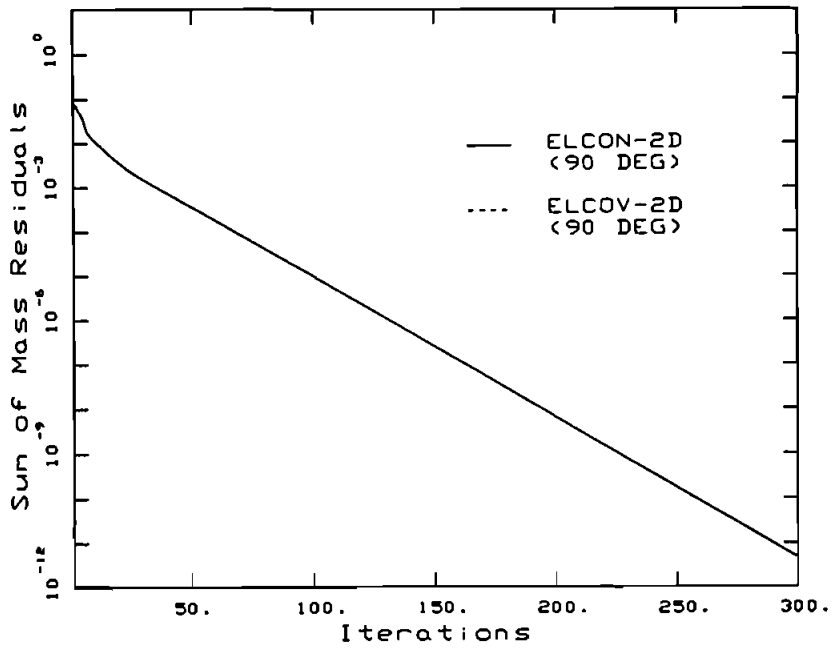

(*a*)

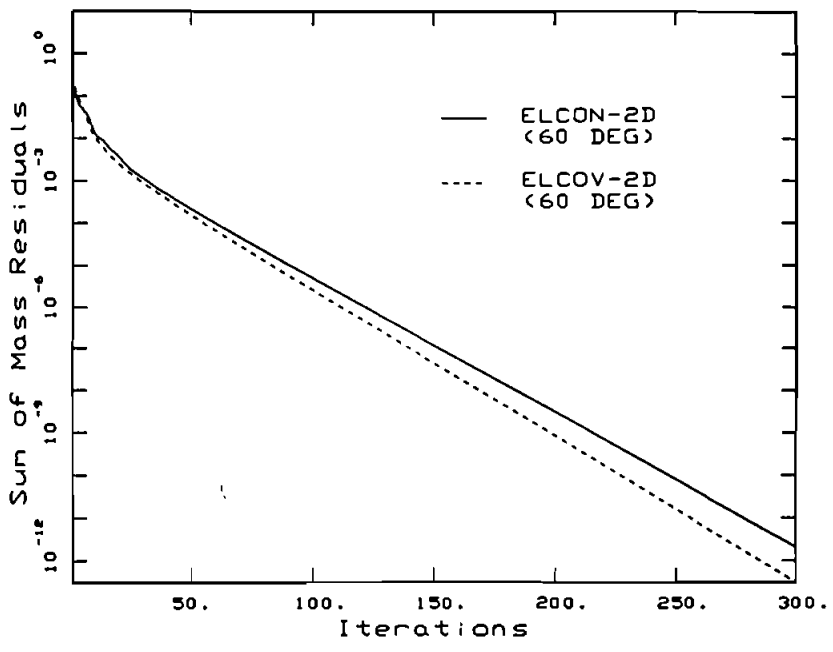

(*b*)

Fig. 10 Convergence histories: (*a*) $\alpha = 90°$, (*b*) $\alpha = 60°$.

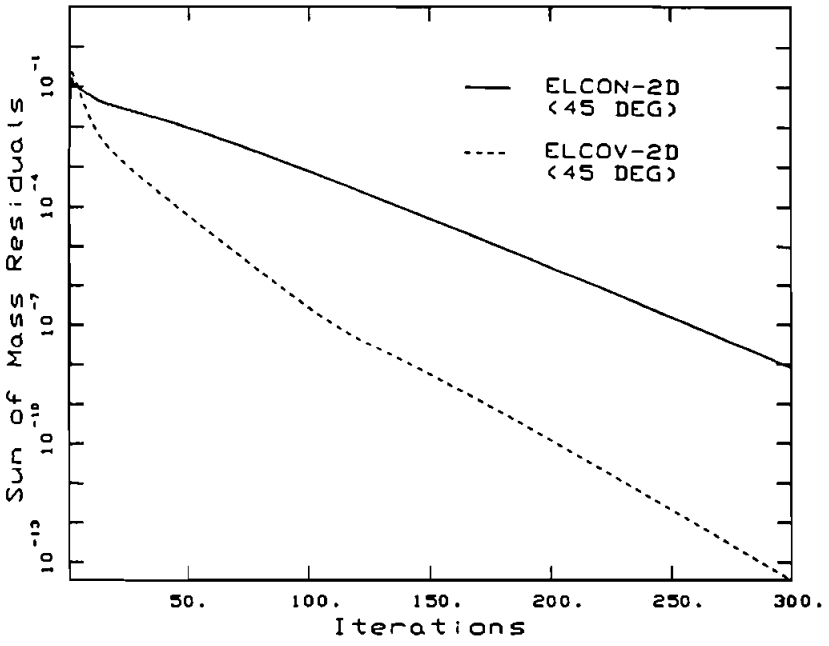

(c)

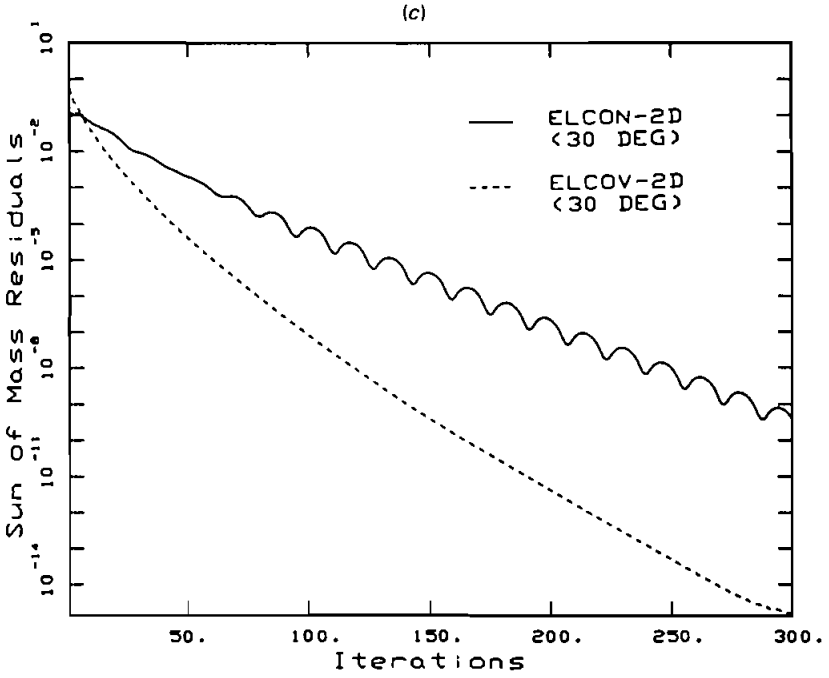

(d)

Fig. 10 Convergence histories (*Continued*): (*c*) $\alpha = 45°$, (*d*) $\alpha = 30°$.

grids are strongly nonorthogonal ($\alpha = 30°$), the ELCON2D code, based on the contravariant cell face velocities, causes some stability problems; convergence is achieved only in a limited range of relaxation factors ($\alpha_p < 0.2$ when $\alpha_u = \alpha_v = 0.7$). A similar experience was also reported in Peric [21] for the same problem as in the present study. Figure 10*d* shows the convergence histories for $\alpha_u = \alpha_v = 0.7$, $\alpha_p = 0.2$, and some wiggles are observed. As mentioned before, the poor performance of the ELCON2D code in strongly nonorthogonal grid situations originates from neglect of nonorthogonal pressure-correction terms in the contravariant velocity-correction equation. However, the inclusion of nonorthogonal pressure-correction terms leads to a nine-point pressure-correction equation in a two-dimensional situation, which adds complexity to the solution procedure. This disadvantage will be particularly grave in practical three-dimensional situations.

CONCLUSIONS

A calculation procedure for incompressible flows in complex geometries based on the modified Rhie and Chow scheme is presented. The relative performance of the scheme based on the covariant cell face velocities and that scheme based on the contravariant cell face velocities is examined through applications to several test problems. The following conclusions can be drawn from these numerical experiments.

1. The accuracy of the converged solution is not affected by the choice of cell face velocities even in a relatively coarse grid situation.
2. When the computational grid is not severely nonorthogonal, the convergence behavior is also not affected by the choice of cell face velocities.
3. When the grid nonorthogonality becomes more significant, better convergence behavior is observed when the covariant velocity components are selected as cell face velocities. The scheme based on the contravariant cell face velocities shows poor convergences as well as unstable solution behavior due to neglect of the nonorthogonal pressure-correction terms.

The scheme based on the covariant cell face velocities shows better solution behavior for all the problems considered in the present study and does not add any significant complexities to the overall solution procedure. As long as efficient solvers for the complicated pressure or pressure-correction equations that include the nonorthogonal terms are not devised, the present covariant cell velocities-based scheme may be a good choice for incompressible flow calculations.

REFERENCES

1. K. C. Karki, A Calculation Procedure for Viscous Flows at All Speeds in Complex Geometries, Ph.D. thesis, University of Minnesota, Minneapolis, 1986.
2. C. R. Maliska and G. D. Raithby, A Method for Computing Three-Dimensional Flows Using Nonorthogonal Boundary-Fitted Coordinates, *Int. J. Numer. Meth. Fluids*, vol. 4, pp. 519–537, 1984.
3. W. Shyy, S. S. Tong, and S. M. Correa, Numerical Recirculation Flow Calculations Using a Body-Fitted Coordinate System, *Numer. Heat Transfer*, vol. 8, pp. 99–113, 1985.

4. K. C. Karki and S. V. Patankar, Calculation Procedure for Viscous Incompressible Flows in Complex Geometries, *Numer. Heat Transfer,* vol. 14, pp. 295–307, 1988.
5. C. M. Rhie and W. L. Chow, Numerical Study of Turbulent Flow Past an Airfoil with Trailing Edge Separation, *AIAA J.*, vol. 21, no. 11, pp. 1525–1532, 1983.
6. M. Peric, A Finite-Volume Method for the Prediction of Three-Dimensional Fluid Flow in Complex Ducts, Ph.D. thesis, University of London, 1985.
7. M. Majumdar, Role of Underrelaxation in Momentum Interpolation for Calculation of Flow with Nonstaggered Grids, *Numer. Heat Transfer,* vol. 13, pp. 125–132, 1988.
8. T. F. Miller and F. W. Schmidt, Use of a Pressure-Weighted Interpolation Method for Solution of the Incompressible Navier-Stokes Equations on a Nonstaggered Grid System, *Numer. Heat Transfer,* vol. 14, pp. 213–233, 1988.
9. W. Rodi, S. Majumdar, and B. Schonung, Finite-Volume Methods for Two-Dimensional Incompressible Flows with Complex Boundaries, *Comput. Meth. Appl. Mech. Eng.*, vol. 75, pp. 369–392, 1989.
10. S. V. Patankar, *Numerical Heat Transfer and Fluid Flow,* Hemisphere, Washington, DC, 1980.
11. M. H. Kobayashi and J. C. F. Pereira, Calculation of Incompressible Laminar Flows on a Nonstaggered, Nonorthogonal Grid, *Numer. Heat Transfer, Part B,* vol. 19, pp. 243–262, 1991.
12. G. D. Thiart, Finite-Difference Scheme for the Numerical Solution of Fluid Flow and Heat Transfer Problems on Nonstaggered Grids, *Numer. Heat Transfer, Part B,* vol. 17, pp. 43–62, 1990.
13. M. H. Kobayashi and J. C. F. Pereira, Numerical Comparisons of Momentum Interpolation Methods and Pressure-Velocity Algorithm Using Nonstaggered Grids, *Commun. Appl. Numer. Meth.*, vol. 7, pp. 173–186, 1991.
14. S. Majumdar, W. Rodi, and S. P. Vanka, On the Use of a Nonstaggered Pressure-Velocity Arrangement for Numerical Solution of Incompressible Flows, Report SFB 210/T/35, University of Karlsruhe, 1987.
15. C. Prakash and S. V. Patankar, A Control-Volume-Based Finite-Element Method for Solving the Navier-Stokes Equations Using Equal-Order Velocity-Pressure Interpolation, *Numer. Heat Transfer,* vol. 8, pp. 259–280, 1985.
16. C. Prakash, An Improved Control-Volume Finite-Element Method for Heat and Mass Transfer and for Fluid Flow Using Equal-Order Velocity-Pressure Interpolation, *Numer. Heat Transfer,* vol. 9, pp. 253–276, 1986.
17. G. E. Schneider and M. J. Raw, Control-Volume Finite-Element Method for Heat Transfer and Fluid Flow Using Collocated Variables—1. Computational Procedure, *Numer. Heat Transfer,* vol. 11, pp. 363–390, 1987.
18. M. Napolitano and P. Orlandi, Laminar Flow in Complex Geometry: A Comparison, *Int. J. Numer. Meth. Fluids,* vol. 5, pp. 667–683, 1985.
19. M. Peric, Analysis of Pressure-Velocity Coupling on Nonorthogonal Grids, *Numer. Heat Transfer, Part B,* vol. 17, pp. 63–82, 1990.

Received 12 August 1991
Accepted 23 January 1992